Atmos. Chem. Phys. Discuss., 12, 5519–5550, 2012
www.atmos-chem-phys-discuss.net/12/5519/2012/
doi:10.5194/acpd-12-5519-2012

Atmospheric Chemistry and Physics Discussions

Modes in the size distributions and neutralization extent of fog-processed ammonium salt aerosols observed at Canadian rural locations

X. H. Yao[1] **and L. Zhang**[2]

[1]Key Lab of Marine Environmental Science and Ecology, Ministry of Education, Ocean University of China, Qingdao 266100, China
[2]Air Quality Research Division, Science and Technology Branch, Environment Canada, 4905 Dufferin Street, Toronto, Ontario, M3H 5T4, Canada

Received: 26 January 2012 – Accepted: 12 February 2012 – Published: 21 February 2012

Correspondence to: L. Zhang (leiming.zhang@ec.gc.ca)

Published by Copernicus Publications on behalf of the European Geosciences Union.

Abstract

Among the 192 samples of size-segregated water-soluble inorganic ions collected using a Micro-Orifice Uniform Deposit Impactor (MOUDI) at eight rural locations in Canada, ten samples were identified to have gone through fog processing. The supermicron particle modes of ammonium salt aerosols were found to be the fingerprint of fog processed aerosols. However, the patterns and the sizes of the supermicron modes varied with ambient temperature (T) and particle acidity and also differed between inland and coastal locations. Under $T > 0\,^{\circ}$C condition, fog-processed ammonium salt aerosols were completely neutralized and had a dominant mode at 1–2 µm and a minor mode at 5–10 µm if particles were in neutral condition, and ammonium sulfate was incompletely neutralized and only had a 1–2 µm mode if particles were in acidic conditions. Under $T < 0\,^{\circ}$C at the coastal site, fog-processed aerosols exhibited a bi-modal size distribution with a dominant mode of incompletely-neutralized ammonium sulfate at about 3 µm and a minor mode of completely-neutralized ammonium sulfate at 8–9 µm. Under $T < 0\,^{\circ}$C condition at the inland sites, fog-processed ammonium salt aerosols were sometimes completely neutralized and sometimes incompletely neutralized, and the size of the supermicron mode was in the range from 1 to 5 µm. Overall, fog-processed ammonium salt aerosols under $T < 0\,^{\circ}$C condition were generally distributed at larger size (e.g., 2–5 µm) than those under $T > 0\,^{\circ}$C condition (e.g., 1–2 µm).

1 Introduction

Similar to clouds, fog plays important roles in the formation of secondary atmospheric aerosols. Fog events modify the size distribution, chemical composition and thus optical properties of preexisting atmospheric aerosols (Ondov and Wexler, 1998; Moore et al., 2004; Fahey et al., 2005; Sun et al., 2006; Aikaw et al., 2007; Herckes et al., 2007; Biswas et al., 2008; Collett Jr. et al., 2008; Dall'Ostol et al., 2009; Kaul et al., 2011;

ACPD
12, 5519–5550, 2012

Rehbein, et al., 2011; Yu et al., 2011). Fog droplets could efficiently scavenge atmospheric gaseous and particulate pollutants, followed by chemical reactions occurring in droplets (Pandis et al., 1990; Collett Jr. et al., 1999, 2008; Fahey et al., 2005; Biswas et al., 2008). When fog dissipates, fog droplets evolve into atmospheric aerosol particles with modified physical and chemical properties. Due to the high deposition velocity of large fog droplets (Herckes et al., 2007), it is difficult to characterize the size-distribution of fog-processed aerosols. Knowledge of size distribution and chemical composition of fog-processed aerosols are limited and factors determining these aerosol properties are poorly understood (Law and Stohl., 2007; Yu et al., 2011).

Enhanced particle pollution was recently reported due to fog-processing events (Sun et al., 2006; Biswas et al., 2008; Yu et al., 2011). High number concentration of fog droplets was observed at sizes 5–6 µm of diameter in polluted ambient air environment (Quan et al., 2011). The small fog droplet size observed in Quan et al. (2011) could be caused by the high fog condensation nuclei (FCN) concentration, similar to the cloud formation under polluted environment (Zhang et al., 2006; Rosenfeld et al., 2008; Qian et al., 2009). These smaller fog droplets should have longer residence time than larger droplets (20–35 µm) as reported by Frank et al. (1998) and Herckes et al. (2007). It is not clear if fog-processing of aerosols enhance particulate pollution in relatively clean environments such as Canadian remote locations, what types of preexisting aerosols are precursors of FCN, and which factors determine physical and chemical properties of fog-processed aerosols.

The purpose of the present study is to identify fog processed aerosols from a suite of field measurements collected at seven rural inland sites and one coastal site in Canada (Zhang et al., 2008a, b) and to explore the variability in size distribution of the fog-processed ammonium salt aerosols with particular attention to the impacts of temperature, particle acidity condition, and preexisting aerosols serving as FCN. Sources and/or formation mechanisms of supermicron particle modes of ammonium salts are investigated in terms of gas-particle condensation, primary emissions, fog processing of aerosols, and heterogeneous reactions of gases with sea-salt aerosols. The results

ACPD
12, 5519–5550, 2012

are expected to improve our understanding on the size distribution of fog-processed ammonium salt aerosols.

2 Methodology

2.1 Data

In this study, an eleven-stage MOUDI (Model 110) with 50 % cut-off points for the particle aerodynamic diameters: 18, 9.9, 6.2, 3.1, 1.8, 1.0, 0.54, 0.32, 0.18, 0.093, and 0.048 µm, were used for sampling at eight rural Canadian in eastern and central Canada (Fig. 1). Simultaneously, a $PM_{2.5}$ sampler equipped with a Na_2CO_3-coated and a citric-acid-coated denuders was also used to collect SO_2, HNO_3 and NH_3 gases and $PM_{2.5}$. Inorganic ions in particles were determined by an ion chromatograph while organics were not measured. In addition, SO_2, NO_x, NO_y and O_3 analyzers were used to measure their concentrations in minutes. On-site meteorological data were recorded to support data analysis. Fog events were judged by on-site observed relative humidity and the record obtained from the nearest meteorological station to the sampling sites (http://www.wunderground.com/history). Detailed information about the sampling sites and chemical analysis can be found in Zhang et al. (2008a, b) and Yao and Zhang (2011).

2.2 Hypothesis 1: Fingerprint of fog-processed aerosols

Among the total of 192 MOUDI samples, ten samples (about 5 % of total data samples) had one or two supermicron particle modes of ammonium salts (colored lines in Fig. 2). However, supermicron particle modes of ammonium salts were absent in non-fog samples (dashed lines in Fig. 2). The difference between fog samples and non-fog samples was statistically significant. Our hypothesis is that the supermicron modes of ammonium salts were the result of fog processing of ammoniated sulfate and/or nitrate. These ten samples having supermicron particle modes of completely-neutralized

ACPD
12, 5519–5550, 2012

or incompletely-neutralized ammonium salts were not likely related to cloud processing of aerosols due to the two considerations: (1) cloud-processed aerosols usually have a fingerprint of the 0.6–1.0 µm mode (Ondov and Wexler, 1998, Yao et al., 2003; Huang et al., 2006); and (2) partially cloud or overcast weather conditions occurred in over 60 % days in a year based on the weather records at airports of eastern Canada, yet only 5 % samples were found to have supermicron ammonium salt aerosols. If cloud processing indeed led to the supermicron modes of ammonium salt aerosols, there should be a lot more samples than the 10 samples identified.

Gas-particle condensation alone usually leads to a particle mode at 0.2 ± 0.1 µm in mass spectra and this formation mechanism does not likely lead to the supermicron modes of ammonium salt aerosols. In another 10 % of samples which might have gone through foggy days, fog-processed aerosols cannot be clearly identified due to the absence of the supermicron modes of ammonium salts. One explanation could be due to the high efficiency of fog in removing particles from ambient air at that time and the amount of fog-processed aerosols was too small to be detectable. Thus, only the 10 samples were used to examine the hypothesis in the present study.

2.3 Hypothesis 2: Impact of acidity on fog-processed aerosols

The ambient acidity condition can affect chemical composition, and possibly, size distribution, of fog-processed aerosols. For example, if ambient condition is acidic, fog-processed aerosols could theoretically be acidic and contain less nitrate, chloride and semi-volatile weak organic acids, and vice versa. Strong acidic, less acidic and neutral fog droplets have been reported under different ambient conditions (Kelmm et al., 1994; Collett Jr. et al., 1999; Moore et al., 2004; Biswas et al., 2008; Sträter et al., 2010; Watanabe et al., 2010; Yao et al., 2011). These studies also showed that NO_3^- can co-exist with SO_4^{2-} and NH_4^+ in fog droplets, regardless of acidity conditions because of a large quality of liquid water. However, when those fog droplets in low pH evaporated, the formed aerosols could be acidic and contain much less amount of

ACPD
12, 5519–5550, 2012

nitrate through evaporation of HNO_3 gas. The hypothesis that the ambient acidity conditions affect chemical composition and size distributions of fog-processed aerosols will be examined here. The relative acidity (RA) is calculated using all observed ion species (in their equivalent concentrations, Kerminen et al., 2001):

$$RA = \frac{NH_4^+ + Na^+ + Ca^{2+} + Mg^{2+} + K^+}{SO_4^{2-} + NO_3^- + Cl^-}$$

Considering that analytical errors of ionic concentrations were about 5 %, RA $\leq$ 0.9 was thereby considered a threshold to judge the presence of acidic aerosols in this study. The missing RA in this study is due to concentrations of the major ion being close to the detection limit when the relative analytical error could be large.

2.4 Hypothesis 3: Impact of ambient temperature on fog-processed aerosols

Because most physical and chemical processes strongly depend on T, its potential impact on size and composition of fog-processed aerosols is worth examining. Freezing fog could occur under $T < 0^{\circ}C$ and frozen fog could occur under $T < -35^{\circ}C$. Frozen fog was also reported with T in the -1 to $-12^{\circ}C$ range, e.g., in the inland areas of the Pacific Northwest (http://en.wikipedia.org/wiki/Fog). Corbin et al. (2012) recently reported that combustion particles could be important ice nuclei in ambient air. In both freezing and frozen fog, ice crystals could be present. When fog dissipates, ice crystals might still exist, depending on ambient conditions. In addition, freezing T could lower rates of chemical reactions and favor semi-volatile species partitioning more in the particle phase (Seinfeld and Pandis, 2006). Thus, size distributions of aerosol particles produced from freezing or frozen fog could be different than those from $T > 0^{\circ}C$. This hypothesis will be examined in this study.

Based on the knowledge discussed above, the presentation of the data analysis is categorized into $T > 0^{\circ}C$ and $T < 0^{\circ}C$ conditions. In the $T > 0^{\circ}C$ regime, data were further subcategorized into neutrality fog-processed aerosols and acidic fog-processed

ACPD
12, 5519–5550, 2012

aerosols (Sects. 3.1 and 3.2, respectively). In the $T < 0\,^{\circ}C$ regime, the fog-processed aerosols at a coastal site were substantially different from those at inland sites and thus coastal and inland site are discussed separately (in Sects. 3.3 and 3.4, respectively).

3 Results and discussion

3.1 Under $T > 0\,^{\circ}C$ and neutrality conditions

The samples collected at an inland site (SPR) on 16–17 November and on 17–18 November 2004 contained a significant amount of SO_4^{2-} and NO_3^- in both submicron and supermicron particles (Fig. 3a, c). Fog occurred from 9 p.m. on 16 November to 10 a.m. on 17 November and from 5 p.m. on 17 November to 9 a.m. on 18 November by judging from the measured $RH > 95\,\%$ and the weather record at the nearest meteorological station (http://www.wunderground.com/history). Fog was observed at stations within a radius of over 100 km during the two days, this fog event was considered to be regional. The RAs (0.95–1.03) narrowly oscillated around unity in different size bins of the two samples (Fig. 3b, d), suggesting that the SO_4^{2-} and NO_3^- were completely neutralized. In the aerosols <3 µm, about 90 % of the SO_4^{2-} and NO_3^- were associated with NH_4^+. In the aerosols >3µm, there was still about 70 % of the SO_4^{2-} and NO_3^- associated with NH_4^+ and the remaining less than 30 % appeared to be associated with metal ions. The neutrality aerosols were supported by the elevated concentrations of NH_3 gas (Table 1). The evidently elevated concentrations of NO_2 and NO_z as well as NH_3 (Table 1) also favored formation of ammonium nitrate.

The size distributions of ions in the sample collected on 16–17 November 2004 was first examined in detail. When log-normal functions were used to fit the size distributions of SO_4^{2-} and NO_3^-, both SO_4^{2-} and NO_3^- exhibited a tri-modal size distribution, i.e., 0.4–0.5, 1.6–1.7 and 8.2–9.0 µm (Fig. S1a, b). The 0.4–0.5 µm mode of SO_4^{2-} and NO_3^- have been well documented as primary emissions (Ondov and Wexler, 1998; Yao

ACPD
12, 5519–5550, 2012

et al., 2003, 2007; Huang and Yu, 2008; Lan et al., 2011), but the two supermicron modes of ammoniated sulfate and nitrate aerosols (ASNA) were rarely reported. The mass ratio of NO_3^-/SO_4^- at the 0.4–0.5 µm mode was lower than at the two supermicron modes (Fig. 3c), indicating that coexistence of ASNA in the submicron mode with ASNA in the two supermicron modes was thermodynamically unfavorable.

The 1–2 µm mode aerosols were once reported (Dall'Ostol et al., 2009; Nie et al., 2010) and could be associated with fog processing (Ondov and Wexler, 1998); but no direct evidence is available to support this assumption. This can only be demonstrated by excluding all the other possible formation routes as discussed below. (1) The sum of ($[Ca^{2+}]+[Na^+]+[K^+]$) in equivalent concentration at the 1.6–1.7 µm mode accounted for only about 10 % of the sum of ($[SO_4^{2-}]+[NO_3^-]$), heterogeneous reactions of acidic gases with crustal, sea-salt and biomass burning aerosols cannot explain most of (SO_4^{2-} + NO_3^-) at this size range. The same was true for the 8.2–9.0 µm mode in which the sum of ($[Ca^{2+}]+[Na^+]+[K^+]$) in equivalent concentration accounted for only about 30 % of the sum of ($[SO_4^{2-}]+[NO_3^-]$). (2) Theoretically, it was less likely for hygroscopic growth of ASNA at the 0.4–0.5 µm mode, together with uptake of SO_2(gas), HNO_3(gas) and NH_3(gas), to the 1.6–1.7 µm mode of ASNA (Kerminen and Wexler, 1995). In the central and eastern Canada, organic carbon only accounted for one-fourth to one-third of the sum of ($[SO_4^{2-}]+[NO_3^-]+[NH_4^+]$) in mass concentration (Jeong et al., 2011) and should play a minor in particle growth. However, it was practically impossible to grow ASNA from 0.4–0.5 µm to 8.2–9.0 µm because it needed an impractical growth factor of 20. In fact, the hygroscopic growth factor of $(NH_4)_2SO_4$ was only 2 at relative humidity of 98 % (Matsumura and Hayashi, 2007). In order to reach the growth factor of 20, a 0.4–0.5 µm ammonium salt aerosol particle needed to be coated by ammonium nitrate which mass should be about three orders of magnitude higher than that of the 0.4–0.5 µm particle. Supersatuation weather condition was thereby needed for the growth, which was present in fog events. Thus, fog processing of SO_4^{2-} and NO_3^- seems to be the only possible path leading to the two supermicron models of ASNA.

ACPD
12, 5519–5550, 2012

Frank et al. (1998) reported that fog droplets sometimes had bi-modal size distribution in number concentrations and sometimes exhibited a uni-modal pattern, although the causes were not well understood. Bi-modal ASNA observed in this study were possibly from evolution of bi-modal fog droplets. However, the FCN associated with the 8.2–9.0 µm mode of ASNA should be different from those associated with the 1.6–1.7 µm mode of ASNA because of different chemical composition between the two modes (Fig. 3a, c).

It was obvious, in the submicron size, that the concentrations of ASNA overwhelmed those of biomass burning, crustal and sea-salt aerosols. Thus, the preexisting ASNA from 1 µm down to 0.05 µm could be one of the major sources of FCN. Yao et al. (2011) reported that ASNA were usually internally mixed with organics in eastern Canada. Although the mass concentration of organics in submicron particles was significantly lower than the sum of those of inorganic ions (Jeong et al., 2011), organics were reported to enhance the efficiency of inorganic aerosols as fog or cloud condensation nuclei (Ming and Russell, 2004; Asa-Awuku et al., 2011; Gierlus et al., 2012). Aerosols <0.05 µm needs an impractically high supersaturation condition to be activated (Dusek et al., 2006) and could not play a significant role in forming FCN. The sum of ($[K^+]$+$[Na^+]$) in equivalent concentration was one order of magnitude smaller than that of NH_4^+. The role of K^+ and Na^+ was thereby negligible for the 8–9 µm mode aerosols. The concentrations of Ca^{2+} and NH_4^+ in the particles >3 µm were at the same order of magnitude. Preexisting Ca^{2+}-contained aerosols could be an important source of FCN under supersatutaion conditions (Koehler et al., 2009; Gierlus et al., 2012) and contributed to the observed 8–9 µm mode aerosols. Moore et al. (2004) reported that the mean ratio of Ca^{2+} in large fog droplets (about 30 µm) to small fog droplets (about 10 µm) was 4.4 at Whiteface Mountain, New York site, but the ratios for SO_4^{2-}, NO_3^- and NH_4^+ oscillated around unity. The higher concentration of Ca^{2+} at about 30 µm fog droplets should be due to the direct activation of Ca^{2+} aerosols, while any other atmospheric processes would favor higher Ca^{2+} at about 10 µm fog droplets. When large fog droplets evaporated into aerosols, the formed aerosols should be large in size and

ACPD
12, 5519–5550, 2012

contained low concentrations of SO_4^{2+}, NO_3^- and NH_4^+ due to small number concentrations of fog droplets. The above mechanism explains the observed 1.6–1.7 µm and 8.2–9.0 µm mode aerosols collected on 16–17 November 2004 at SPR.

The concentrations of coarse particle NO_3^- are generally much lower than fine particle NO_3^- in cold seasons, as was the case for most of the samples collected in cold seasons (Zhang et al., 2008a). However, in this particular sample, the concentration of the 1.6 µm mode NO_3^- is higher than that of the 0.5 µm mode (Fig. 3a), indicating that fog increased the concentration of particulate NO_3^- in the coarse mode in the atmosphere. This also implies that the new formation of nitrate in fog droplets was likely more than the removal of nitrate through deposition of fog droplets and interstitial aerosols. The elevated concentrations of gas precursors of NO_3^- support this hypothesis (Table 1). It is also noted that the SO_4^{2-} concentrations at the 1.7 µm and 9.0 µm modes were much lower than those at the 0.4 µm mode, suggesting that the new formation of ammonium salt aerosol was mostly ammonium nitrate and that the new formation of SO_4^{2-} in fog droplets was slower than the deposition of SO_4^{2-} in fog droplets and interstitial coarse particles.

We further examined size distributions and composition of ions in the samples collected on 17–18 November 2004 at SPR. Three modes of SO_4^{2-} were observed at 0.3, 1.0 and 5.0 µm while NO_3^- had only two modes at 1.0 µm and 5.0 µm (Fig. S2a, b). The 0.3 µm mode was between the upper limit of the condensation mode and the lower limit of primary aerosols (Ondov and Wexler, 1998). Following the analysis presented earlier, formation of ASNA at the 1.0 µm and 5.0 µm modes was also probably ascribed to fog-processing of aerosols. In this sample, Ca^{2+}-contained aerosols played a negligible role as FCN because of a much lower concentration of Ca^{2+}. The same can be said for K^+-contained and Na^+-contained aerosols. FCN could be mainly activated from preexisting ammoniated sulfate aerosols and/or their mixture with organics in the submicron size. Condensation and coagulation possibly grew the FCN into bi-modal pattern fog droplets and eventually evaporated into bi-modal aerosols. The different

ACPD
12, 5519–5550, 2012

ratios of NO_3^-/SO_4^{2-} between the 1.0 µm mode and the 5.0 µm mode aerosols also suggested that the two modes of aerosols were likely evolved from different types of fog droplets.

The concentration of SO_4^{2-} in the 1.0 µm aerosols was slightly higher than that in the 0.3 µm mode aerosols, suggesting that the formation rate of SO_4^{2-} in fog droplets was slightly higher than its deposition rate. The concentrations of NO_3^- or NH_4^+ in the 1.0 µm mode aerosols were evidently higher than those in the 0.3 µm mode aerosols, indicated that fog probably increased concentrations of those species in the atmosphere.

3.2 Under $T > 0\,^{\circ}C$ and acidic conditions

One sample collected at the coastal site (KEJ) and two samples collected at one inland site (CHA) meets the conditions of $T > 0\,^{\circ}C$ and acidic particles. Size distributions of ionic species and RA in the sample collected at Kejimkujik (KEJ) during 10–11 November 2002 were shown in Fig. 4a, b, and fog occurred from 6 p.m. on November to 12 a.m. on 11 November and was also considered as a regional event based on the record from ground weather stations. Since the site is situated at a coastal area, non-sea-salt-SO_4^{2-} (nss-SO_4^{2-}) was thereby used in the analysis. Three modes of nss-SO_4^{2-} were observed at 0.3, 1.5 and 3.7 µm (Fig. S3a). The RA values between 0.3–2 µm were less than 0.8, indicating that the nss-SO_4^{2-} was incompletely neutralized. Under such acidic condition, the hygroscopic growth together with SO_2 oxidation to nss-SO_4^{2-} cannot grow the 0.3 µm mode nss-SO_4^{2-} to the 1.5 µm mode nss-SO_4^{2-} according to a theoretical analysis by Kerminen and Wexler (1995). In addition, the sum of Ca^{2+} and K^+ in the aerosols between 0.3–2 µm only accounted for less than 5 % of the nss-SO_4^{2-} in equivalent concentration. Thus, heterogeneous formation of nss-SO_4^{2-} on Ca^{2+} and K^+ contained aerosols at the size range were unimportant. A significant high concentration of sea-salt aerosols was present at 3–5 µm (Fig. 4a). Heterogeneous formation of nss-SO_4^{2-} or sulfuric acid gas condensation process should have produced higher

ACPD
12, 5519–5550, 2012

concentration of nss-SO_4^{2-} at the 3–5 µm mode than the 1–2 µm mode. However, the 3.7 µm mode nss-SO_4^{2-} was close to the detection limit, much lower than the concentration of the 1.5 µm mode. It is thus concluded that fog processing of nss-SO_4^{2-} most probably occurred, leading to the 1.5 µm mode of nss-SO_4^{2-}.

It is interesting to note that the concentration of nss-SO_4^{2-} at the 1.5 µm mode was less than that at the 0.3 µm mode. This might be due to the low conversion rate of SO_2 to SO_4^{2-} under acidic condition in fog droplets. However, it was also possible that fog-processed nss-SO_4^{2-} were diluted, leading to a lower concentration of nss-SO_4^{2-} at the 1.5 µm mode.

In acidic environment, incompletely-neutralized sulfate aerosols inhibited the formation of ammonium nitrate (Seinfeld and Pandis, 2006) and the NO_3^- can exist only as metal salts. Therefore, the concentration of NO_3^- in the aerosols between 0.3–2 µm was negligible because of lack of metal ions in this size range. The NO_3^- dominated at the 2.9 µm mode (Fig. S3b). However, Na^+ and Cl^- dominated at the 3.7 µm mode (Fig. S3c). The maximum surface area concentration of sea-salt aerosols is usually located at a smaller size compared to the size of the maximum mass concentration of sea-salt aerosols. Thus, NO_3^- formed through surface reactions between acidic gases and sea-salt aerosols would peak at smaller sizes than that of the maximum sea-salt mass concentrations. The similar observations were reported by Zhuang et al. (1999) and Zhao and Gao (2008).

The two samples collected at Chalk River (CHA) on 14–15 June 2004 and 16–20 June 2004 are shown in Fig. 5. Fog occurred from 10 p.m. on 14 June to 5 a.m. on 15 June from 9 a.m. to 11 a.m. on 16 June, and from 1 a.m. to 4 a.m. on 19 June, all of which appeared to be local fog events since no fog was recorded at a station 20 km away from the site. For the sample collected during 14–15 June 2004, the RAs in the particles less than 3.1 µm varied from 0.80 to 0.87 except one outlier (with a value of 1.34) at the size bin of 0.32–0.54 (Fig. 5b), which was caused by suspected high concentration of Ca^{2+} (Fig. 5a) because the rest of the size bins had extremely low

ACPD
12, 5519–5550, 2012

concentration (e.g., less than one tenth of the size bin of 0.32–0.54 µm). The small RAs suggest that ammoniated sulfate aerosols were incompletely neutralized. SO_4^{2-} and NH_4^+ were two dominant ionic species and NO_3^- was negligible in the acidic aerosols. Three modes of SO_4^{2-} were obtained at 0.4, 1.4 and 6.0 µm, respectively (Fig. S4a). The incompletely neutralized ammoniated sulfate aerosols at the 1.4 µm mode were probably ascribed to fog-processing events as discussed above. Compared to SO_4^{2-} in the submicron mode, the supermicron models of SO_4^{2-} had evidently lower concentrations under acidic conditions. The size distributions and chemical composition in the sample collected on 16–20 June 2004 were almost the same as those collected on 14–15 June 2004, except without an outlier of Ca^{2+} at the at the size bin of 0.32–0.54 µm (Fig. 5c, d and Fig. S4b). These two samples were expected to have gone through similar fog conditions.

3.3 At a coastal site under $T < 0\,^{\circ}C$ condition

Two samples collected at the coastal site (KEJ) likely encountered fog, one sample was collected during 8–9 November 2002 (Fig. 6a, b) and another during 9–10 November 2002 (Fig. 6c, d). The ambient temperature ranged from −2.6 to −8.8 °C during the fist sample period (Table 1) and fog occurred from 5 a.m. to 8 a.m. on 8 November by judging from the measured RH. This fog seemed to be a local event. In this sample, nss-SO_4^{2-} and NH_4^+ were two dominant ionic species in the particle <3 µm where the RA varied from 0.7 to 0.9, suggesting that the ammoniated sulfate aerosols were incompletely neutralized. The low NH_3 concentration of 0.2 ppb (Table 1) favored formation of incompletely-neutralized sulfate aerosols and inhibited formation of ammonium nitrate.

Four modes of nss-SO_4^{2-} were obtained at 0.2, 0.6, 2.9 and 8.0 µm, respectively during the first sample (Fig. S5a), with the dominant mode at 2.9 µm. The two submicron modes can be explained by known mechanism such as condensational growth and cloud processing (Ondov and Wexler, 1998; Zhuang et al., 1999; Yao et al., 2003; Lan

ACPD
12, 5519–5550, 2012

et al., 2011). The 2.9 µm mode nss-SO_4^{2-} was mainly associated with NH_4^+ because the amount of other metal ions accounted for only a small fraction of the nss-SO_4^{2-}. Under the acidic condition found in this sample, the above mentioned mechanism cannot explain the dominant mode at 2.9 µm of nss-SO_4^{2-} associated with NH_4^+, and the most likely process behind this was fog-processing. Preexisting incompletely-neutralized ammonium sulfate and their mixture with organics in the submicron size could be the major FCN which eventually led to the 2.9 µm mode of nss-SO_4^{2-}. Fog processing of aerosols apparently increased the concentration of nss-SO_4^{2-} in the atmosphere as evident by the higher nss-SO_4^{2-} concentration at the 2.9 µm mode than those at the submicron sizes.

Also in this sample, NO_3^- had a dominant mode at 8 µm and a minor condensation mode at 0.2 µm (Fig. S5b). As mentioned earlier, nss-SO_4^{2-} also had a minor mode at 8 µm in which nss-SO_4^{2-} was apparently associated with NH_4^+. The 8 µm mode of NO_3^- was apparently associated with Na^+ because 1) the Na^+ also had a unique mode at 8 µm; and 2) the equivalent ratio of ($[NO_3^-]+[Cl^-]$)/($[Na^+]$) was in the range of 1.18–1.22, close to the ratio of $[Cl^-]/[Na^+]$ in sea water, which is 1.17. The fresh/aged sea-salt aerosols could be the major source of the FCN which eventually led to the 8 µm mode aerosols. It was reported that sea spray bubble aerosol could also contain organics and the later could enhance efficiency of CCN (Russell et al., 2009; Moore et al., 2011). On the other hand, the primary sea-salt aerosols usually had a mode at 2–5 µm in mass concentration worldwide. The re-suspended road dust was not likely the major source of the 8 µm mode of Na^+ because of the negligible Ca^{2+} (Fig. 6a) and the wind speed of about 1–2 m s^{-1} did not favor re-suspension of road dust. Fog droplets derived from sea spray aerosols could scavenge ammoniated sulfate preexisting in the atmosphere and uptake SO_2 and NH_3 gases, leading to nss-SO_4^{2-} at the 8 µm mode. The RA indicated that the 8 µm mode nss-SO_4^{2-} was completely neutralized (Fig. 6b).

The second sample collected on 9–10 November at KEJ was the sample immediately after the first sample was collected on 8–9 November. The ambient temperature ranged

ACPD
12, 5519–5550, 2012

from −1.7 to 7.5 °C (Table 1) and regional fog occurred from 5 p.m. on 9 November to 11 a.m. on 10 November. Similar to the findings in sample 1, nss-SO_4^{2-} also had four modes at 0.2, 0.7, 2.8 and 8.0 µm, respectively (Fig. 6c, d, Fig. S6a). The mechanisms forming the supmicron modes of nss-SO_4^{2-} in this sample were likely the same as those in sample 1 discussed above. NO_3^- and Na^+ also peaked at the same mode in this sample, but at 3.9 µm (Fig. S6b, c) instead of 8 µm as observed in sample 1. It is noticed that most samples (fog processed or non-fog events) during this campaign had a mode of 4–7 µm for Na^+ (Zhang et al., 2008a). Thus, modes at different size ranges can be formed for NO_3^- with or without fog processing process.

3.4 At inland sites under $T < 0$ °C condition

The high concentrations of SO_4^{2-} and NO_3^- on 19–20 February 2003 at Algoma (ALG) (Fig. 7a) indicated that the polluted air plume affected the site. However, the low ambient temperature ranging from −5.2 to −8.8 0 °C did not favor the formation of secondary aerosols. Fog occurred from 3 p.m. on 19 February to 11 a.m. on 20 February and appeared to be a local event. Three modes of SO_4^{2-} occurred at 0.3, 0.7 and 4.5 µm while four modes of NO_3^- occurred at 0.2, 0.7, 4.5 and 8 µm (Fig. S7a, b). The RA at the 0.32–0.54 µm was 0.88, suggesting that the SO_4^{2-} at the size bin were incompletely neutralized. The RA varied from 0.96 to 1.14 at other size bins, suggesting that the SO_4^{2-} and NO_3^- were completely neutralized.

The incompletely-neutralized ammoniated sulfate aerosols at the 0.3 µm mode was likely from primary sources and the NO_3^- at 0.2 µm mode and the ASNA at the 0.7 µm mode were due to secondary formation processes. The NO_3^- at the 8 µm mode was found to be associated with Ca^{2+} and the 8 µm mode was not detected for SO_4^{2-}. Thus, the 8 µm mode NO_3^- was likely due to heterogeneous reactions between acidic gases with crustal aerosols rather than fog-processing of NO_3^-.

None of the above processes can lead to the 4.5 µm mode of ASNA, except fog processing as explained below. The sum of ([Ca^{2+}]+[Na^+]+[K^+]) accounted for only about

ACPD
12, 5519–5550, 2012

10 % of the sum of ($[SO_4^{2-}]$+$[NO_3^-]$); heterogeneous reactions between acidic gases and crustal, sea-salt and biomass burning aerosols cannot explain the observed (SO_4^{2-} + NO_3^-) at the 4.5 µm mode. The mass ratios of NO_3^-/SO_4^{2-} at the 0.7 µm and 4.5 µm modes were basically the same. Assuming that the 0.7 µm mode ASNA grows into the 4.5 µm mode ASNA, a growth factor of 6.5 is needed and can only be reached under supersatuation conditions. Moreover, fog also appeared to significantly lower concentrations of ASNA in the atmosphere by inferring a substantial decrease of ASNA's concentration at the 4.5 µm mode, comparing their concentrations to the submicron particles.

No fog occurred during the period of 12:40 to 18:10 local time on 6 March 2002 at Egbert (EGB); however, regional fog lasted for four hours before sampling when the ambient temperature was at −4 °C. A mode at 3.1–3.5 µm was observed for ASNA in this sample (Fig. 7c, d and Fig. S8ab). Crustal and sea-salt ions accounted for only 20–30 % of the sum of ($[SO_4^{2-}]$ +$[NO_3^-]$) at this mode while the remaining 70–80 % of the sum of ($[SO_4^{2-}]$ + $[NO_3^-]$) were apparently associated with NH_4^+. Heterogeneous reactions were also not likely the major cause of the SO_4^{2-} and NO_3^- at this mode. The ASNA at this mode was most likely the result of fog processing of aerosols as supported by the discussions below.

Very high concentration of HNO_3 gas (1.7 ppb, Table 1) was observed during the sampling period. The value was even higher than the maximum daily averaged concentration of HNO_3 gas observed in winter in urban areas of North America cities, e.g., Toronto (Godri et al., 2009) and New York (Ren et al., 2006), even under high NO_2 concentration conditions. Photochemical formation of HNO_3 in the gas-phase under such cold conditions and low NO_2 concentrations at EGB should not be able to produce the observed high concentration of HNO_3 gas. Besides, the mass ratio of NO_3^- to SO_4^{2-} at the 3.1–3.5 µm mode was substantially lower than the ratio in submicron sizes (Fig. 7c). All of these evidences pointed to the possibility that a large quantity of HNO_3 was released into the gas phase when fog droplets evolved into aerosols. On

ACPD
12, 5519–5550, 2012

this occasion, fog droplets were probably acidic. This hypothesis was also supported by the RA (0.88) at the 1.8–3.2 µm size bin. RAs at other supermicron size bins were in the range of 1.0 and 1.03, which could be explained by the released of HNO_3 that decreased the particle acidity. Thus, the post process of fog processing during this sampling period was a source of HNO_3 gas.

Comparing samples discussed in this section with those in Sect. 3.1, it is found that fog processed aerosols under $T < 0\,^{\circ}C$ condition were generally distributed at larger size (e.g., 2–5 µm) than those under $T > 0\,^{\circ}C$ condition (e.g., 1–2 µm). It is speculated that ice could be present in fog-processed aerosols under T<0°C condition, leading to the 2–5 µm mode. It is noticed that one sample collected on 9–10 December 2004 at SPR with T in the range of −2.9 to 1.7 °C had similar size distribution and composition of fog-processed SO_4^{2-} (Fig. 8a, b and Fig. S9) to some of the samples collected under $T > 0\,^{\circ}C$ and acidic conditions. In this sample, fog occurred from 5 p.m. on 9 December to 8 a.m. on 10 December and appeared to be a local event. Ice was not likely present in this particular sample since the temperature was only slightly below zero during part of the sampling period.

4 Conclusions

Fog-processed aerosols observed at Canadian inland and coastal rural sites were identified and factors determining their size distributions and chemical composition were investigated. The supermicron modes of ASNA were identified as the fingerprint of fog-processing. Consistent with previous studies, fog processing could lead ammonium salt aerosols to a mode of 1–2 µm. This study further identified that fog processing could also lead ammonium aerosols at modes of 2–5 µm and 5–10 µm. The ammonium salt was in the form of sulfate under acidic condition and in the form of sulfate and nitrate under other conditions.

Temperature was found to be an important parameter in determining size distributions of fog-processed aerosols. When $T > 0\,^{\circ}C$, size distributions and chemical

ACPD
12, 5519–5550, 2012

composition of fog-processed aerosols also strongly rely on acidity condition. (1) Under the neutrality condition, ASNA had two modes at the 1–2 µm and 5–10 µm, respectively. ASNA at the 1–2 µm mode was likely the result of preexisting submicron aerosols being activated as FCN which eventually evolved into aerosols. In addition to preexisting submicron aerosols, Ca^{2+}-conatined supermicron aerosols could also be activated as FCN, contributing to the 5–10 µm mode of ASNA. Moreover, fog apparently increased concentrations of ASNA in the atmosphere under such condition. (2) Under the acidic condition, fog-processing of ammoniated sulfate, which was incompletely neutralized, had a mode at 1–2 µm. Preexisting submicron aerosols could be the major contributor of FCN while concentrations of Ca^{2+}-conatined aerosols were too low to be important. The concentrations of SO_4^{2-} and NH_4^+ at the 1–2 µm were lower than those at submicron size in these acidic samples, suggesting that fog probably played a role in lowering concentrations of these species.

When $T < 0^{\circ}C$, fog-processed nss-SO_4^{2-} at a coastal site exhibited a bi-modal size distribution (the dominant mode at 2.8–2.9 µm and a minor mode at 8.0 µm). The nss-SO_4^{2-} at the 2.8–2.9 µm mode was incompletely neutralized and was apparently evolved from fog droplets being activated from submicron nss-SO_4^{2-} aerosols. The nss-SO_4^{2-} at the 8.0 µm mode was completely neutralized and was evolved from fog droplets being activated from fresh/aged sea-salt aerosols. Fog-processed nss-SO_4^{2-} at inland sites had a unique mode at 3–5 µm or 1–2 µm where nss-SO_4^{2-} sometimes was completely neutralized and sometimes not. At low T, Ca^{2+}-contained supermicron aerosols were likely not FCN and the 5–10 µm mode of fog-processed aerosols were absent.

Fog processing was found to modify submicron NH_4NO_3 aerosols and release a large quantity of HNO_3 gas under acidic conditions. This process substantially lowered the residence time of reactive nitrogen in the atmosphere because of the much higher deposition rate of HNO_3 gas than that of submicron NH_4NO_3 aerosols, and is worth further investigation.

ACPD
12, 5519–5550, 2012

Supplementary material related to this article is available online at: http://www.atmos-chem-phys-discuss.net/12/5519/2012/acpd-12-5519-2012-supplement.pdf.

Acknowledgements. We appreciate R. Vet, A. Wiebe, C. Mihele, S. Iqbal for data collection and data quality control and Yujiao Zhu for providing assistance in figure preparation.

References

Aikawa, M., Hiraki, T., Suzuki, M., Tamaki, M., and Kasahara, M.: Separate chemical characterizations of fog water, aerosol, and gas before, during, and after fog events near an industrialized area in Japan, Atmos. Environ., 41, 1950–1959, 2007.

Asa-Awuku, A., Moore, R. H., Nenes, A., Bahreini, R., Holloway, J. S., Brock, C. A., Middlebrook, A. M., Ryerson, T. B., Jimenez, J. L., DeCarlo, P. F., Hecobian, A., Weber, R. J., Stickel, R., Tanner, D. J., and Huey, L. G.: Airborne cloud condensation nuclei measurements during the 2006 Texas Air Quality Study, J. Geophys. Res., 116, D11201, doi:10.1029/2010JD014874, 2011.

Biswas, K. F., Ghauri, B. M., and Husain, L.: Gaseous and aerosol pollutants during fog and clear episodes in South Asian urban atmosphere, Atmos. Environ., 42, 7775–7785, 2008.

Corbin, J. C., Rehbein, P. J. G., Evans, G. J., and Abbatt, J. P. D.: Combustion particle as ice nuclei in an urban environnent: evidence from single-particle mass spectrometry, Atmos. Environ., doi:10.1016/j.atmosenv.2012.01.007, in press, 2012.

Collett Jr., J. L., Hoag, K. J., Rao, X., and Pandis, S. N.: Internal acid buffering in San Joaquin Valley fog drops and its influence on aerosol processing, Atmos. Environ., 33, 4833–4847, 1999.

Collett Jr., J. L., Herckes, P., Youngster, S., and Lee, T.: Processing of atmospheric organic matter by California radiation fogs, Atmos. Res., 87, 232–241, 2008.

Dall'Osto, M., Harrison, R. M., Coe, H., and Williams, P.: Real-time secondary aerosol formation during a fog event in London, Atmos. Chem. Phys., 9, 2459–2469, doi:10.5194/acp-9-2459-2009, 2009.

ACPD
12, 5519–5550, 2012

Dusek, U., Frank, G. P., Hildebrandt, L., Curtius, J., Schneider, J., Walter, S., Chand, D., Drewnick, F., Hings, S., Jung, D., Borrmann, S., and Andreae, M. O: Size matters more than chemistry for cloud-nucleating ability of aerosol particles, Science, 312, 1375–1378, 2006.

Fahey, K. M., Pandis, S. N., Collett Jr., J. L., and Herckes, P.: The influence of size-dependent droplet composition on pollutant processing by fogs, Atmos. Environ., 39, 4561–4574, 2005.

Frank, G., Martinsson, B. G., Cederfelt, S., Berg, O. H., Swietlick, E., Wendisch, M., Yuskiewicz, B., Heitzenberg, J., Wiedensohler, A., Orsini, D., Stratmann, F., Laj, P., and Ricci, L.: Droplet formation and growth in polluted fogs, Contr. Atmos. Phys., 71, 65–85, 1998.

Gierlus, K. M., Laskina, O., Abernathy, T. L., and Grassian, V. H.: Laboratory study of the effect of oxalic acid on the cloud condensation nuclei activity of mineral dust aerosol, Atmos. Environ. 46, 125–130, 2012.

Herckes, P., Chang, H., Lee, T., and Collett Jr. J. L. : Air pollution processing by radiation fogs, Water Air Soil Poll., 181, 65–75, 2007.

Huang, X.-F., Yu, J. Z., He, L.-Y., and Yuan, Z. B.: Water-soluble Organic Carbon and Oxalate in Aerosols at a Coastal Urban Site in China: Size Distribution Characteristics, Sources and Formation Mechanisms, J. Geophys. Res, 111, D22212, doi:10.1029/2006JD007408, 2006.

Huang, X.-F. and Yu, J. Z.: Size distributions of elemental carbon in the atmosphere of a coastal urban area in South China: characteristics, evolution processes, and implications for the mixing state, A tmos. Chem. Phys., 8, 5843–5853, doi:10.5194/acp-8-5843-2008, 2008.

Jeong, C.-H., McGuire, M.L., Herod, D., Dann, T., Dabek-Zlotorzynska, E., Wang, D., Ding, L., Celo, V, Mathieu, D. and Evans, G. J.: Receptor model based identification of $PM_{2.5}$ sources in Canadian cities, Atmos. Pollution Res., 2, 158–171, 2011.

Kaul, D. S., Gupta, T., Tripathi, S. N., Tare, V., and Collett, Jr. J. L.: Secondary organic aerosol: a comparison between foggy and nonfoggy days, Environ. Sci. Technol., 45, 7307–7313, 2011.

Kerminen V.-M. and Wexler, A. S.: Enhanced formation and development of sulfate particles due to marine boundary-layer circulation, J. Geophys. Res., 100, 23051–23062, 1995

Kerminen, V.-M., Hillamo, R., Teinilä, K.Pakkanen, T., Allegrini, I., and Sparapani, R.: Ion balances of size resolved tropospheric aerosol samples: implications for the acidity and atmospheric processing of aerosols, Atmos. Environ., 35, 5255–5265, 2001.

Klemm, O., Bachmeier, A. S., Talbot, R. W., and Klemm, K. I.: Fog chemistry at the New England coast: Influence of air mass history, Atmos. Environ., 28, 1181–1188, 1994.

ACPD
12, 5519–5550, 2012

Koehler, K. A., Kreidenweis, S. M., DeMott, P. J., Petters, M. D., Prenni, A. J., Carrico, C. M.: Hygroscopicity and cloud droplet activation of mineral dust aerosol, Geophys. Res. Lett., 36, L08805, 5 pp., doi:10.1029/2009GL037348, 2009.

Godri, K. J., Evans, G. J., Slowik, J., Knox, A., Abbatt, J., Brook, J., Dann, T., and Dabek-Zlotorzynska, E.: Evaluation and application of a semi-continuous chemical characterization system for water soluble inorganic $PM_{2.5}$ and associated precursor gases, Atmos. Meas. Tech., 2, 65–80, doi:10.5194/amt-2-65-2009, 2009.

Lan, Z.-J., Chen, D.-L., Li, X., Huang, X.-F., He, L.-Y., Deng, Y.-G., Feng, N., and Hu, M.: Modal characteristics of carbonaceous aerosol size distribution in an urban atmosphere of South China, Atmos. Res., 100, 51–60, 2011.

Law, K. S. and Stohl, A.: Arctic air pollution: origins and impacts, Science, 315, 1537–1540, 2007.

Matsumura, T. and Hayashi, M.: Hygroscopic growth of an $(NH_4)_2SO_4$ aqueous solution droplet measured using an environmental scanning electron microscope (ESEM), Aerosol Sci.Technol., 41, 770–774, 2007.

Ming, Y. and Russell, L. M.: Organic aerosol effects on fog droplet spectra, J. Geophys. Res., 109, D10206, doi:10.1029/2003JD004427, 2004.

Moore, K. F., Sherman, D. E., Reilly, J. E., Collett Jr. J. L.: Drop size-dependent chemical composition in clouds and fogs. Part I. Observations, Atmos. Environ., 38, 1389–1402, 2004.

Moore, M. J. K., Furutani, H., Roberts, G. C., Moffet, R. C., , Gilles, M. K., Palenik, B., and Prather, K. A.: Effect of organic compounds on cloud condensation nuclei (CCN) activity of sea spray aerosol produced by bubble bursting, Atmos. Environ., 45, 7462–7469, 2011.

Nie, W., Wang, T., Gao, X., Pathak, R. K., Wang, X., Gao, R., Zhang, Q., Yang, L., and Wang, W.: Comparison among filter-based, impactor-based and continuous techniques for measuring atmospheric fine sulfate and nitrate, Atmos. Environ., 44, 4396–4403, 2010.

Ondov, J. M. and Wexler, A. S.: Where do particulate toxins reside? An improved paradigm for the structure and dynamics of the urban mid- Atlantic aerosol, Environ. Sci. Tech., 32, 2547–2555, 1998.

Pandis, S. N., Seinfeld, J. H., and Pilinis, C.: Chemical composition differences in fog and cloud droplets of different sizes, Atmos. Environ., 24, 1957–1969, 1990.

Qian, Y., Gong, Y., Fan, J., Leung, L. R., Bennartz, R., Chen, D., and Wang, W.: Heavy pollution suppresses light rain in China: Observations and modeling, J. Geophys. Res., 114, D00K02, doi:10.1029/2008JD011575, 2009.

ACPD
12, 5519–5550, 2012

Quan, J., Zhang, Q., He, H., Liu, J., Huang, M., and Jin, H.: Analysis of the formation of fog and haze in North China Plain (NCP), Atmos. Chem. Phys., 11, 8205–8214, doi:10.5194/acp-11-8205-2011, 2011.

Rehbein, P. J. G., Jeong, C.-H., McGuire, M. L., Yao, X. H., Corbin, J. C., Evans, G. J.: Cloud and fog processing enhanced gas-to-particle partitioning of trimethylamine, Environ. Sci. Technol., 45, 4346–4352, 2011.

Ren, X., Brune, W. H., Mao, J., Mitchell, M. J., Lesher, R. L., Simpas, J. B., Metcalf, A. R., Schwab, J. J., Cai, C., Li, Y., Demerjian, K. L., Felton, H. D., Boynton, G., Adams, A., Perry, J., He, Y., Zhou, X., Hou, J.: Behavior of OH and HO_2 in the winter atmosphere in New York City, Atmos. Environ., 40, S252–S263, 2006.

Rosenfeld, D., Lohmann, U., Raga, G. B., O'Dowd, C. D., Kulmala, M., Fuzzi, S. Reissell, A., and Andreae, M. O.: Flood or drought: how do aerosols affect precipitation?, Science, 321, 1309–1313, 2008.

Russell, L. M., Hawkins, L. N., Frossard, A. A., Quinn, P. K., and Bates, T. S.: Carbohydrate-like composition of submicron atmospheric particles and their production from ocean bubble bursting, PNAS, 107, 6652–6657, 2009.

Seinfeld, J. H. and Pandis, S. N.: Atmospheric chemistry and physics from air pollution to climate change (Second Edition). Willey Interscience, New York, 2006.

Sträter, E., Westbeld, A., and Klemm, O.: Pollution in coastal fog at Alto Patache, Northern Chile, Environ. Sci. Pollut. Res. (International), 17, 1563–1573, 2010.

Sun, Y., Zhuang, G., Tang, A. A., Wang, Y., and An, Z.: Chemical characteristics of $PM_{2.5}$ and PM_{10} in haze-fog episodes in Beijing, Environ. Sci. Technol., 40, 3148–3155, 2006.

Watanabe, K., Honoki, H., Iwai, A., Tomatsu, A., Noritake, K., Miyashita, N., Yamada, K., Yamada, H., Kawamura, H., and Aoki, K.: Chemical characteristics of fog water at Mt. Tateyama, near the coast of the Japan Sea in central Japan, Water Air Soil Poll., 211, 379–393, 2010.

Yao, X. H., Lau, A. P. S., Fang, M., Chan, C. K., and Hu, M.: Size distributions and formation of ionic species in atmospheric particulate pollutants in Beijing, China: 1–inorganic ions, Atmos. Environ., 37, 2991–3000, 2003.

Yao, X. H., Lau, N. T., Fang, M., Chan, C. K.: Size distribution and condensation growth of submicron particles in on-road vehicle plumes in Hong Kong, Atmos. Environ., 41, 3328–3338, 2007.

ACPD
12, 5519–5550, 2012

Yao, X. H. and Zhang, L.: Sulfate formation in atmospheric ultrafine particles at Canadian inland and coastal rural environments, J. Geophys. Res., 116, D10202, 13 pp.., doi:10.1029/2010JD015315, 2011.
Yao, X. H., Rehbein, P. J. G., Lee, C. J., Evans, G. J., Corbin, J., and Jeong, C.-H.: A study on the extent of neutralization of sulphate aerosol through laboratory and field experiments using an ATOFMS and a GPIC, Atmos. Environ., 45, 6251–6256, 2011.
Yu, X., Zhu, B., Yin, Y., Yang, J., Li, Y., and Bu, X.: A comparative analysis of aerosol properties in dust and haze-fog days in a Chinese urban region, Atmos. Res., 99, 241–247, 2011.
Zhang, L., Michelangeli, D. V., and Taylor, P. A.: Influence of aerosol concentration on precipitation formation in low-level, warm stratiform clouds, J. Aerosol Sci., 37, 203–217, 2006.
Zhang, L., Vet, R., Wiebe, A., Mihele, C., Sukloff, B., Chan, E., Moran, M. D., and Iqbal, S.: Characterization of the size-segregated water-soluble inorganic ions at eight Canadian rural sites, Atmos. Chem. Phys., 8, 7133–7151, doi:10.5194/acp-8-7133-2008, 2008a.
Zhang, L., Wiebe, A., Vet, R., Mihele, C., O'Brien, J. M., Iqbal, S., and Liang, Z.:Measurements of reactive oxidized nitrogen at eight Canadian rural sites, Atmos. Environ., 42, 8065–8078, 2008b.
Zhang, Q., Jimenez, J. L., Worsnop, D. R., and Canagaratna, M.: A case study of urban particle acidity and its influence on secondary organic aerosol, Environ. Sci Technol., 41, 3213–3219, 2007.
Zhao, Y. and Gao, Y.: Acidic species and chloride depletion in coarse aerosol particles in the US east coast, Sci. Total Environ., 407, 541–547, 2008.
Zhuang, H., Chan, C. K., Fang, M., and Wexler, A. S.: Formation of nitrate and nonsea-salt sulfate on coarse particles, Atmos. Environ., 33, 4223–4233, 1999.

ACPD
12, 5519–5550, 2012

Table 1. Meteorological conditions [mean (min–max)] and concentrations of gases (ppb) (BDL – below detection limit).

Site	Sampling period	T (°C)	RH (%)	SO_2	HNO_3	NH_3	NO_2	NO_z
SPR	11:40 16 Nov – 9:50 17 Nov 2004	4.8 (3.5–7.4)	83 (73–98)	1.0	0.3	0.6	8.6	1.5
	10:10 17 Nov – 9:00 18 Nov 2004	7.6 (6.5–9.4)	85 (62–98)	0.3	0.2	0.4	10.8	0.9
	9:10 9 Dec – 14:20 10 Dec 2004	−0.9 (−2.4–1.7)	80 (60–98)	0.1	0.1	0.2	1.7	0.5
CHA	9:30 14 June – 9:00 15 June 2004	20.3 (13.6–27.0)	67 (41–97)	0.1	0.1	0.3	0.4	0.8
	9:15 16 June – 9:00 20 June 2004	17.4 (5.5–29.3)	66 (38–96)	0.2	0.4	0.2	0.5	0.6
ALG	11:00 19 Feb – 10:30 20 Feb 2003	−7.2 (−5.2–−8.8)	87 (49–99)	0.1	0.2	BDL	1.3	0.9
EGB	12:40 6 Mar – 18:10 6 Mar 2002	0 (−0.6–0.4)	86 (84–88)	0.8	1.7	0.1	6.3	3.2
KEJ	17:50 8 Nov – 10:20 9 Nov 2002	−6.4 (−8.8–−2.6)	82 (59–98)	0.3	0.04	0.1	1.1	0.8
	11:10 9 Nov – 10:20 10 Nov 2002	3.7 (−1.7–7.5)	92 (68–100)	0.9	0.09	0.2	2.3	0.9
	10:50 10 Nov – 10:40 11 Nov 2002	9.0 (6.5–11.3)	89 (49–100)	0.4	0.06	0.3	BDL	0.6

ACPD
12, 5519–5550, 2012

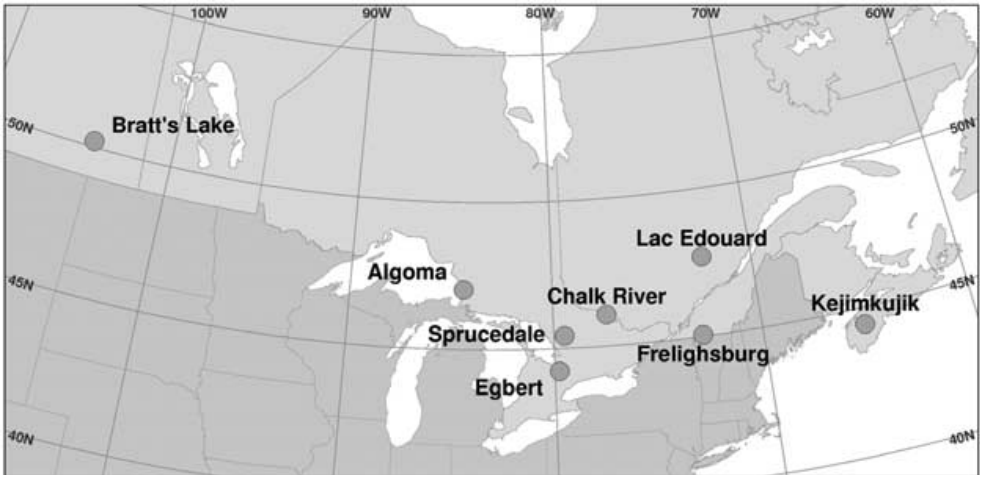

Fig. 1. Map of sampling sites.

ACPD
12, 5519–5550, 2012

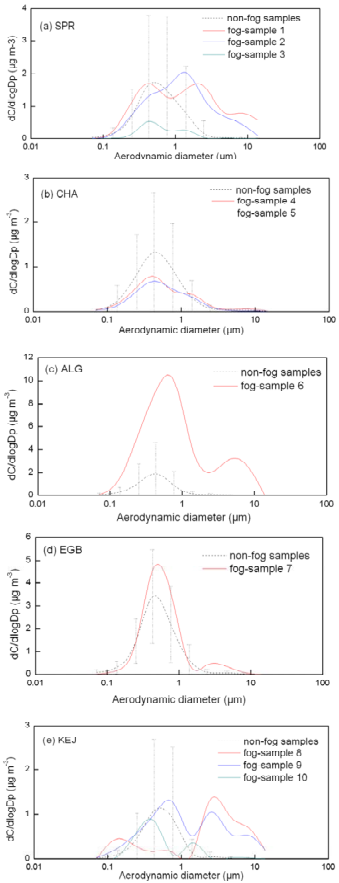

Fig. 2. Mass size distributions of NH_4^+ in fog and non-fog samples: dashed line and error bar represent the average and standard deviation of all non-fog samples in each campaign and each colored line represent one fog-samples defined in Table 1.

ACPD
12, 5519–5550, 2012

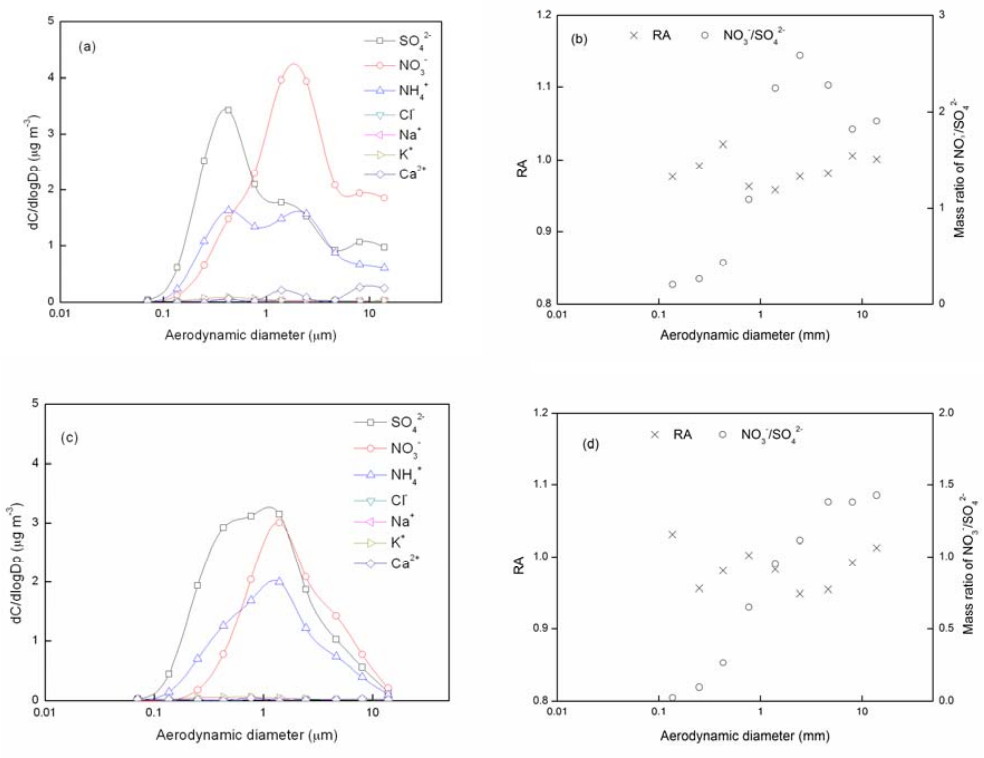

Fig. 3. Size distributions of ionic concentrations, RA and mass ratio of NO_3^-/SO_4^{2-} during the period from 11:40 on 16 November to 9:50 on 17 November 2004 and from 10:10 on 17 November to 9:00 on 18 November 2004 at SPR.

ACPD
12, 5519–5550, 2012

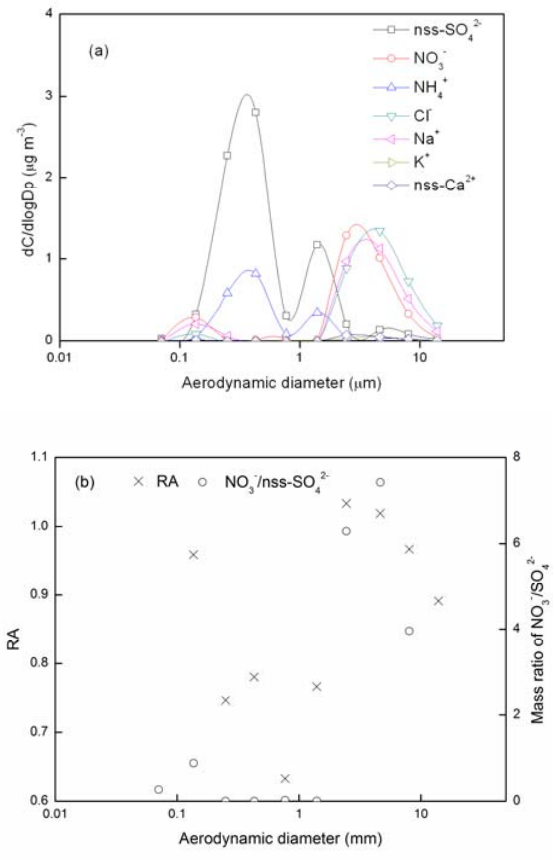

Fig. 4. Size distribution of ionic concentrations, RA and mass ratio of NO_3^-/SO_4^{2-} during the period from 10:50 on 10 November to 10:40 on 11 November 2002 at KEJ.

ACPD
12, 5519–5550, 2012

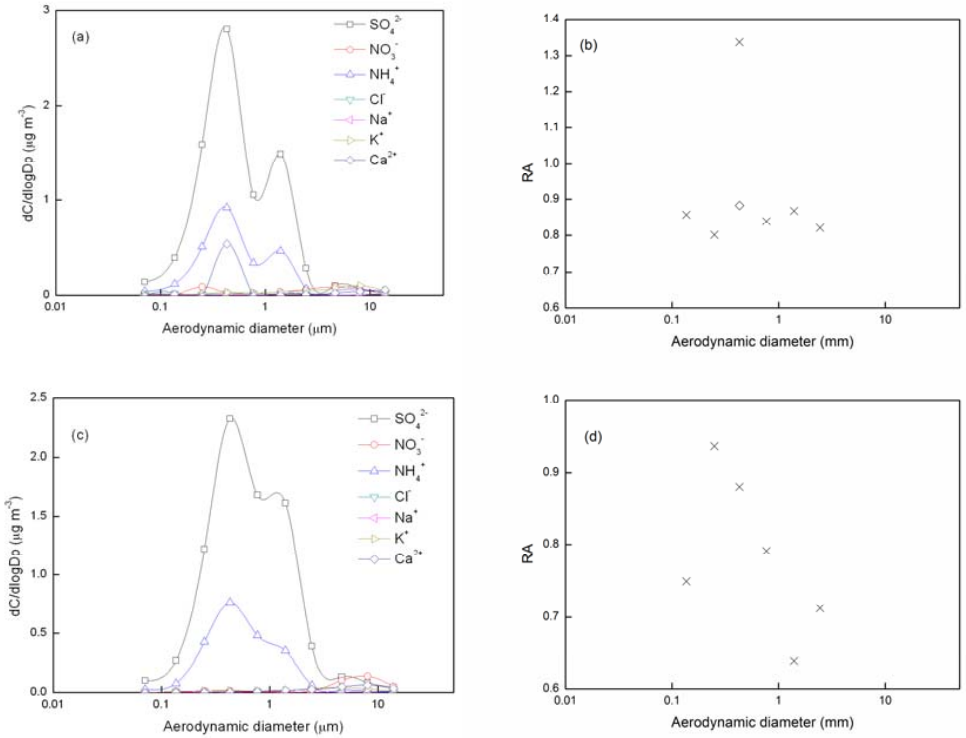

Fig. 5. Size distributions of ionic concentrations and RA during the period from 9:30 on 14 June–9:00 on 15 June 2004 and from 9:15 on 16 June–9:00 on 20 June 2004 at CHA (**a** and **b** represents the sample collected on 14–15 June; **b**: cross represents RA and diamond represents RA in which Ca^{2+} was excluded from the estimation; **c** and **d** represents the sample collected on 16–20 June).

ACPD
12, 5519–5550, 2012

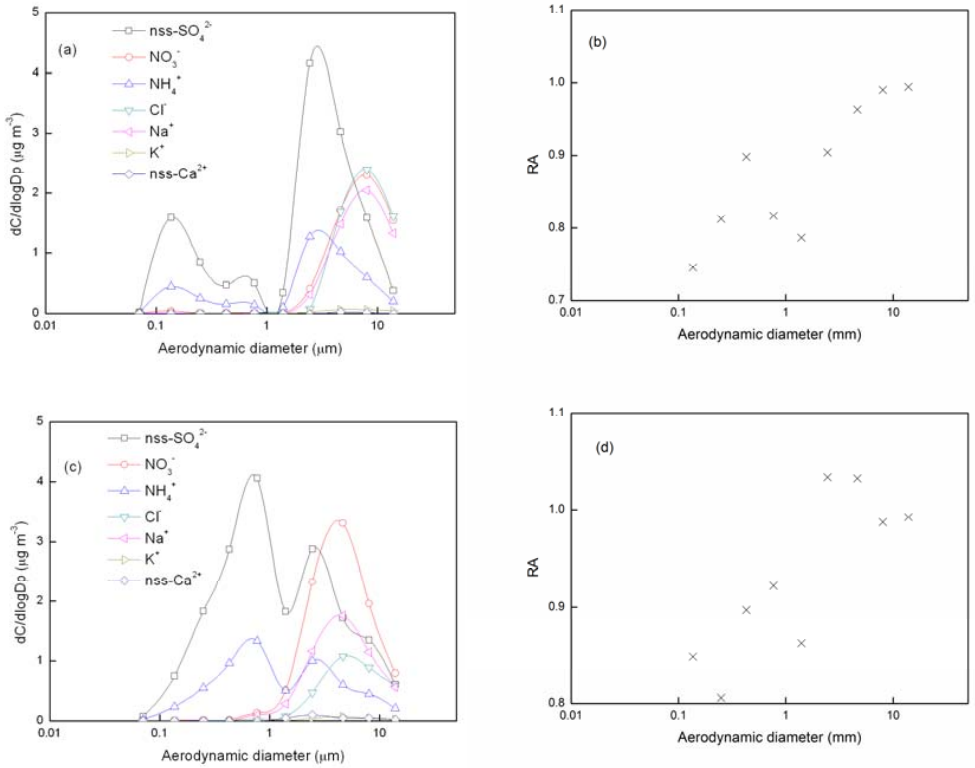

Fig. 6. Size distributions of ionic concentrations and RA during the period from 17:50 on 8 November to 10:20 on 9 November 2002 and from 11:10 on 9 November to 10:20 on 10 November 2002 at KEJ (**a** and **b** represents the sample collected on 8–9 November; **c** and **d** represents the sample collected on 9–10 November).

ACPD
12, 5519–5550, 2012

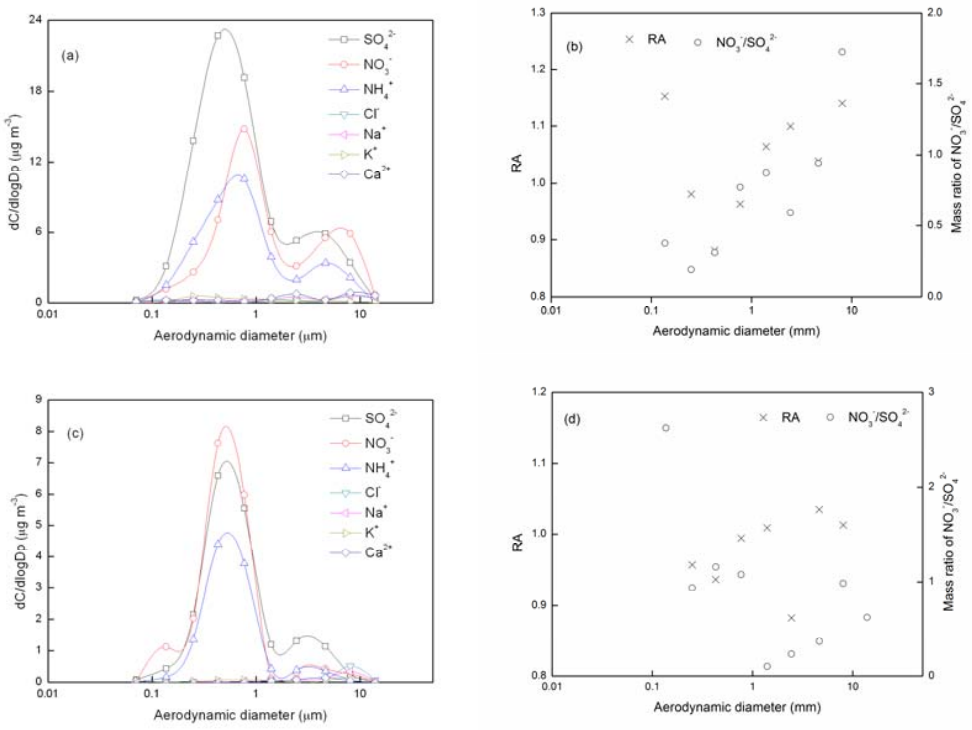

Fig. 7. Size distribution of ionic concentrations, RA and mass ratio of NO_3^-/SO_4^{2-} during the period from 11:00 on 19 February 2003–10:30 on 20 February 2003 at ALG and during the period from 11:40 on 16 November to 9:50 on 17 November 2004 at EGB (ab represented the sample collected at ALG; cd represented the sample collected at EGB).

ACPD
12, 5519–5550, 2012

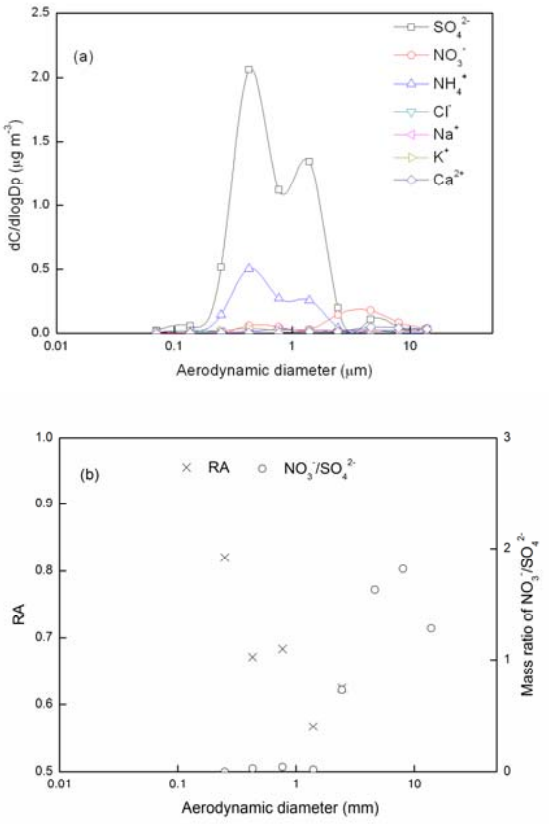

Fig. 8. Size distributions of ionic concentrations and RA during the period from 9:10 on 9 December to 14:20 on 10 December 2004 at SPR.

ACPD
12, 5519–5550, 2012